Mostafa Rassaian
The Boeing Company
Defense and Space Group
Seattle, WA 98124-2499

Power Spectral Density Conversions and Nonlinear Dynamics

To predict the vibration environment of a payload carried by a ground or air transporter, mathematical models are required from which a transfer function to a prescribed input can be calculated. For sensitive payloads these models typically include linear shock isolation system stiffness and damping elements relying on the assumption that the isolation system has a predetermined characteristic frequency and damping ratio independent of excitation magnitude. In order to achieve a practical spectral analysis method, the nonlinear system has to be linearized when the input transportation and handling vibration environment is in the form of an acceleration power spectral density. Test data from commercial isolators show that when nonlinear stiffness and damping effects exist the level of vibration input causes a variation in isolator resonant frequency. This phenomenon, described by the stationary response of the Duffing oscillator to narrow-band Gaussian random excitation, requires an alternative approach for calculation of power spectral density acceleration response at a shock isolated payload under random vibration. This article details the development of a plausible alternative approach for analyzing the spectral response of a nonlinear system subject to random Gaussian excitations. © *1994 John Wiley & Sons, Inc.*

INTRODUCTION

The dynamic behavior of many aerospace vehicles carried as shock isolated payloads can be predicted using a wide range of analytical and numerical methods, such as the finite element technique. However, a key element in any approach is the ability to accurately characterize the stiffness and damping of the shock isolation system. The development of finite element models assumes linear behavior, together with the appropriate discretized structural damping and stiffness representation, for commercially available low frequency shock isolators. The two most widely used analytical solutions are based upon: evaluation of modal frequency response to a given power spectral density input, usually in the form of an acceleration versus frequency spectrum; and evaluation of peak modal frequency response to shock induced environments known as the shock response spectrum analysis.

Experimental data from some commercial isolators show that when nonlinear stiffness and damping effects exist, the level of vibration input causes a variation in isolator resonant frequency. These nonlinear characteristics do not lend themselves to the classic linear frequency response analysis techniques. This phenomenon, which was first introduced by Duffing in Nayfeh and Mook (1979), therefore requires an unconventional approach for the use of power spectral density (PSD) acceleration response at a shock isolated payload under random vibration.

Received October 2, 1992; Accepted October 12, 1993

Shock and Vibration, Vol. 1, No. 4, pp. 349–356 (1994)

CCC 1070-9622/94/040349-08

Using the analytical techniques presented in this article it is possible to avoid costly and time-consuming nonlinear finite element analysis. The basic analytical approach is divided into two distinct phases. Phase 1 develops the actual nonlinear isolator characteristics, and phase 2 develops the methodology for calculating the frequency and damping of the equivalent linear isolation system. Therefore, phase 1 consists of the following steps: construct a nonlinear isolator force element with the appropriate form of damping modeled, that is, hysteretic; use static and dynamic isolator test data for model correlation; and incorporate the validated isolator element into a simple model representing rigid payload masses connected to ground through a nonlinear isolation system.

Phase 2 includes: transform input acceleration PSDs to equivalent acceleration time histories for each studied vibration environment; input individual converted acceleration time histories to the nonlinear rigid payload model and output payload acceleration responses; convert individual payload acceleration time history responses back to PSDs to identify isolation system resonant frequencies (using input/output transfer functions to characterize damping levels) corresponding to each ground or air-induced vibration level; and run the final detailed random vibration response analysis using these derived equivalent linear isolator stiffness and damping characteristics in the more complex isolator/payload finite-element model. The necessary steps taken for simulation of a nonlinear isolator (phase 1) are discussed next.

NONLINEAR ISOLATOR CHARACTERISTICS

Helical wire rope-type isolators are often used to mitigate the shock and vibration environments to sensitive electronic equipment. This type of isolator offers the advantages of being insensitive to a wide range of thermal conditions, as well as being inherently higher damped than most typical elastomeric isolators. This damping is provided by flexure hysteresis, that is, the rubbing and sliding friction between the strands of the wire rope. As discussed in the following paragraphs, testing shows it is the isolator's hysteretic load-deflection behavior that leads to its nonlinear vibration isolation characteristics.

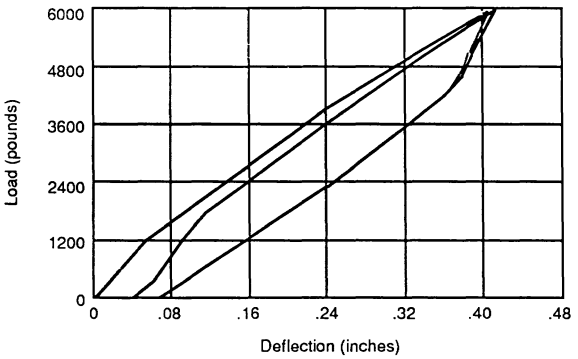

FIGURE 1 Isolator static load-deflection curve.

Static Test

Static testing in the vertical compression direction was performed on a standard universal test machine. The isolator was cycled three times between zero and maximum load. Figure 1 shows the hysteretic load-deflection characteristics of this isolator evident in the test data.

Dynamic Test

Dynamic testing was also performed in the vertical direction. The objective of this test was to characterize resonant frequency and damping values for the isolators supporting a simulated 1-g static load. Two isolators were bolted to the shaker table with the dummy payload mounted above and no lateral restraint. A slow (1 octave/min) vertical sine sweep acceleration input was applied at three amplitudes of 1/4, 1/2, and 1 g from 5 to 160 Hz. The vertical transmissibility across the isolator showed a definite shift in resonant frequency dependent on the magnitude of vibration input. As shown in Fig. 2, the resonant frequency increased from 6.5 to 12.0 Hz as the amplitude of acceleration input decreased from 1.0 to 0.25 g. The corresponding percent critical damping ratio estimated from these curves also showed a slight decrease as input amplitude dropped but still indicated a highly damped system (damping ratio of 20% at 0.25-g input level).

Isolator Model Approach

The model for a two-dimensional axial force element consisting of a linear spring and dashpot in parallel with an elastically connected coulomb damper is shown in Fig. 3. This model is used to simulate a nonlinear wire rope isolator with

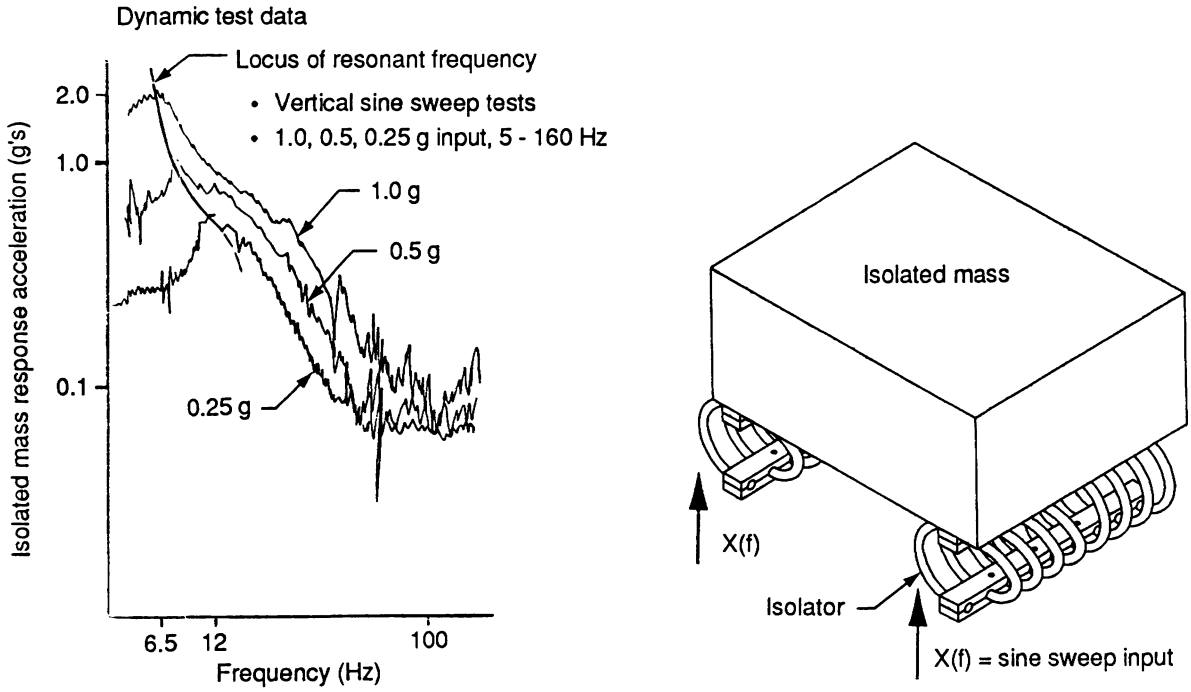

FIGURE 2 Isolator nonlinear stiffness characteristics.

highly hysteretic load-deflection characteristics. The coulomb damper element exhibits linear spring behavior with viscous damping until the specified maximum or minimum force limits are exceeded, at which point axial slipping occurs at a constant force. Unloading of the coulomb element occurs linearly from the point of maximum slip. The superposition of the approximated coulomb damping force and the parallel spring/viscous damping force results in the complete hysteresis function illustrated in Figure 4.

The wire rope isolator model validation uses both static and dynamic test data. Figure 5 demonstrates the isolator model validation using the static hysteretic characteristics of the isolators. Figure 6 presents the comparison of isolator model dynamic response to the dynamic test data at the prescribed excitation vibration levels.

Further analysis using the isolator model shows that the resonant frequency shift with variation in input vibration level is primarily a function of the hysteretic behavior and the influence of the isolator stiffness in the transition region between static load and unload curves.

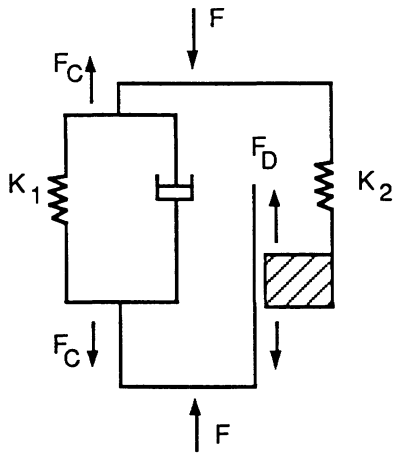

FIGURE 3 Nonlinear isolator model.

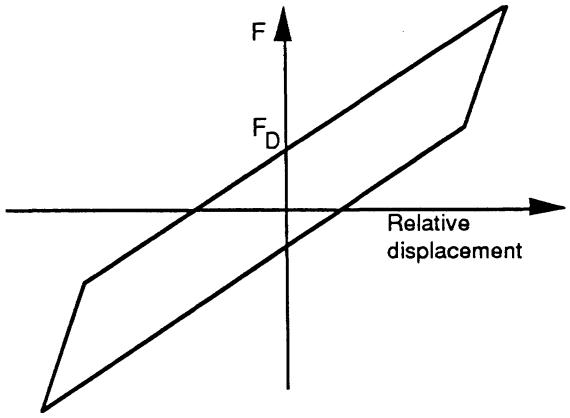

FIGURE 4 Composite isolator force.

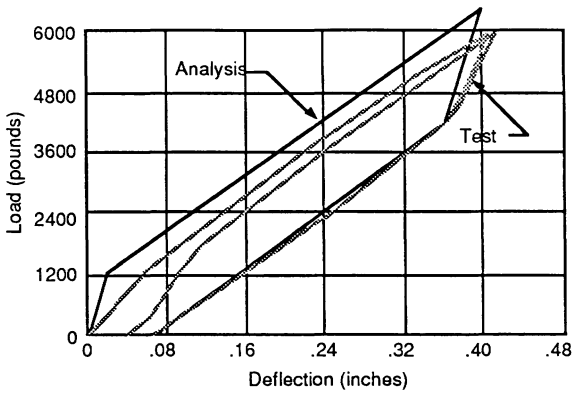

FIGURE 5 Isolator static load-deflection curve (test vs. analysis).

The steps required for calculation of the linear equivalent isolator system (phase 2) are described in the following sections.

PSD CONVERSIONS

As demonstrated by actual test data, payloads supported on wire rope type isolators will display nonlinear response characteristics under normal input vibration levels. For aerospace vehicle applications, the input vibration environments are typically in the form of acceleration PSDs that require a linearity assumption for the entire physical system if modal frequency response analysis of the input is desired. The first step toward establishing an appropriate frequency response function for a nonlinear system is to estimate a sample time domain forcing function from the PSD input spectrum. The time domain forcing function can then be used as input to a two degrees of freedom (DOF) payload model with time history acceleration output. To determine the resonant frequency and the peak gain factor (Q) of the isolator, the acceleration output of the two DOF model can be converted back to a PSD acceleration spectrum and ratioed to the input spectrum. The steps detailing these conversions together with a typical application will be presented here.

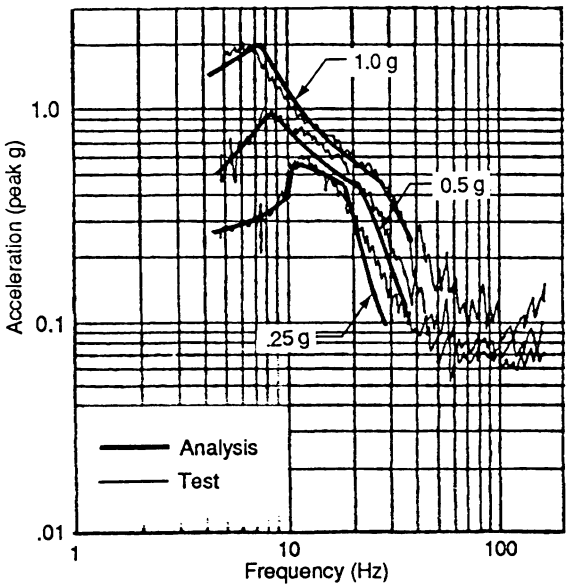

FIGURE 6 Isolator payload dynamic response vs. frequency (test vs. analysis).

PSD Conversion to Time Domain

Given a PSD function $G(f)$ and a total time history record length T, an estimate of the Fourier amplitude $|X(f, T)|$ is given by Bendat and Piersol (1986)

$$|X(f, T)|^2 = \frac{T}{2} G(f). \tag{1}$$

Assume record length T is related to a starting frequency, f_{st} by

$$T = \frac{1}{f_{st}}, \tag{2}$$

also frequency f_i is defined by

$$f_i = \frac{i}{T}, \quad i = 1, 2, \ldots, N, \tag{3}$$

where N represents the number of frequencies in the digitized spectrum.

Let the amplitude $|X|$ and the phase angle σ define the complex Fourier spectrum X here by

$$X(f_i, T) = |X|e^{j\sigma(f_i)}, \quad i = 1, 2, \ldots, N, \tag{4}$$

such that

$$\sigma(f_i) = 2\pi r_i, \quad i = 1, 2, \ldots, N, \tag{5}$$

where j is the complex imaginary number ($j = \sqrt{-1}$). Since the phase angle σ is a random variable, we require that r_i take on uniformly random numbers between 0 and 1 ($0 < r_i < 1$) at each frequency f_i.

The time history spectrum $x(t)$ can now be obtained by the definition

$$x(t) = \int_0^T X(f, T)e^{2\pi jft}\, df. \tag{6}$$

Combining Eqs. (1) and (4) in the discretized form of Eq. (6) will yield a nonergodic random process that consists of cosine sample functions for $x(t)$ such that

$$x(t_k) = \sqrt{\frac{T}{2}} \sum_{i=1}^{N} \sqrt{G(f_i)}\cos(2\pi f_i t_k + \sigma_i), \quad k = 1, \ldots, M, \tag{7}$$

where M represents the number of samples in the time record. Equation (7) constitutes the operation required to convert a PSD spectrum to its equivalent time domain representation. To illustrate the conversion numerically, consider the acceleration PSD environment given in Fig. 7. Figure 8 shows the time history equivalent obtained through this operation. To assure the transformation is accurate, one expects to obtain the same PSD spectrum shown in Fig. 7 starting from its equivalent time history and proceeding in reverse steps. The reverse steps needed to verify the accuracy of the resulting PSD spectrum require finite Fourier transformation that will be discussed next.

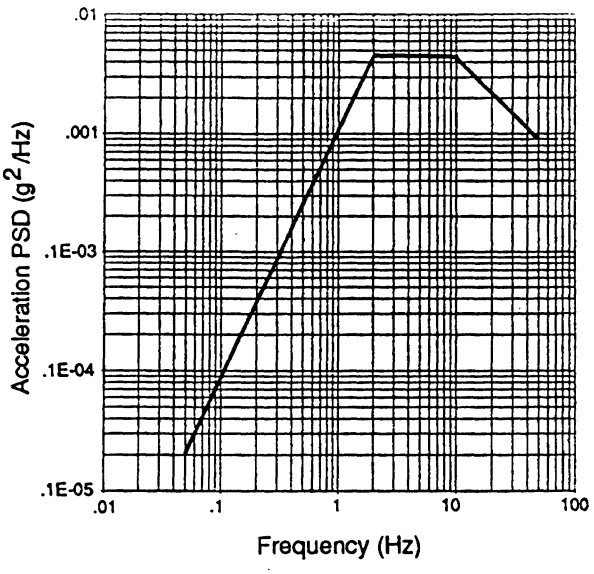

FIGURE 7 Acceleration PSD environment.

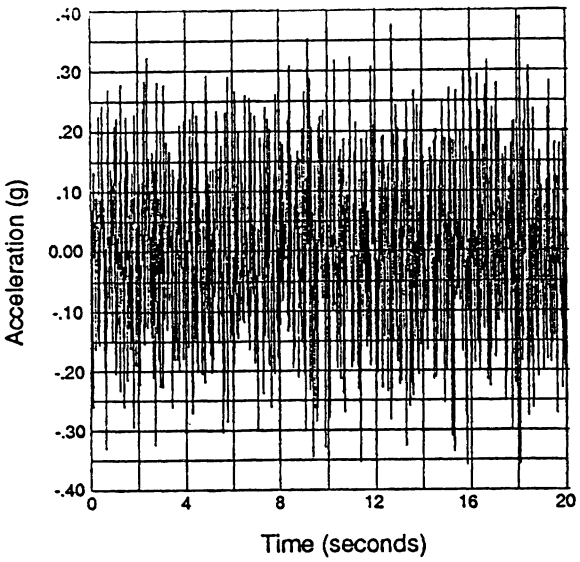

FIGURE 8 Time history acceleration equivalent to PSD input.

Time Domain Conversion to PSD

The proposed method here is to derive spectral density functions based on a finite Fourier transform of the time history data records, which allows checking to assure that the previous transformation from PSD to time domain is acceptable.

Consider $x(t)$ representing a sample time history. For a finite time interval $0 \le t \le T$, define

$$|\bar{X}(f_i, T) = \text{Real}\left\{\int_0^T x(t)e^{-2\pi jf_i t}\, dt\right\}, \quad i = 1, 2, \ldots N. \tag{8}$$

The quantity $|X(f_i, T)|$ represents the amplitude of the finite Fourier transform of $x(t)$. The bar is used to differentiate from the Fourier amplitude in Eq. (1).

Equation (8) can be expressed in the form

$$|\bar{X}(f_i, T)| = \left\{\sum_{k=1}^{M} [x(t_k)\cos 2\pi f_i t_k]^2 + \sum_{k=1}^{M} [x(t_k)\sin 2\pi f_i t_k]^2\right\}^{1/2}, \quad i = 1, 2, \ldots N. \tag{9}$$

The amplitude of the PSD spectrum $\bar{G}(f_i, T)$ can be determined from Eq. (1),

$$|\bar{G}(f_i, T)| = \frac{2}{T}|\bar{X}(f_i, T)|^2,$$

$$i = 1, 2, \ldots, N, \quad (10)$$

in which $|\bar{X}(f_i, T)|$ is defined by Eq. (9).

Now the conversion of time record $x(t)$ to power spectral density form can be obtained using Eqs. (9) and (10). A direct comparison of $|\bar{G}(f_i, T)|$ obtained from $x(t_k)$ to the starting PSD, $|G(f_i, T)|$, is shown in Fig. 9. This comparison shows the ideal Fig. 7 spectrum falls along the average of the Fig. 9 calculation. No averaging is applied to the calculated acceleration spectra. A result closer to Fig. 7 could be obtained by selecting a larger time history record T and applying an averaging technique.

TWO DOF PAYLOAD MODEL

The purpose of the dynamic simulation of the payload and support configuration is to evaluate the payload response to the vibration environment when supported on the nonlinear isolation system.

The number of degrees of freedom necessary are determined by accounting for the principle dynamic mass and interface stiffness properties that cause strong coupling of modes. The use of a minimum number of DOF in the model is desirable because computational efficiency is reduced considerably in the presence of nonlinear elements. For instance it is sufficient to use a two DOF model for obtaining an accurate transmissibility function for the nonlinear wire rope isolator because it only causes a strong coupling with the payload through its linear impedance characteristics. The time-dependent transmissibility function can then be converted to frequency spectra using the methods discussed in the previous section to determine the nonlinear shock isolator element resonant frequency for a given vibration excitation input.

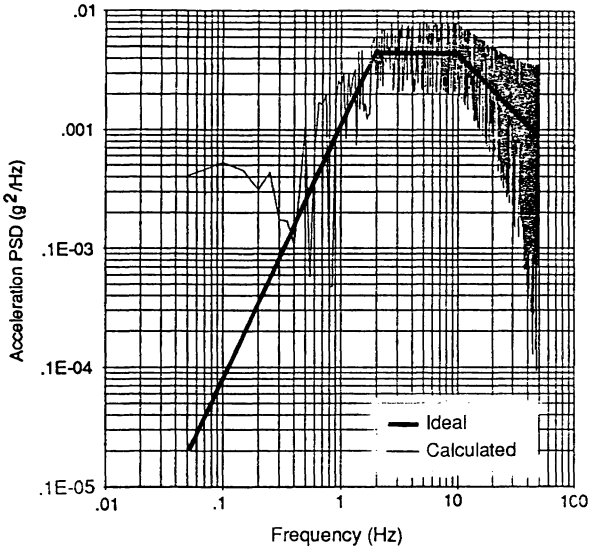

FIGURE 9 Calculated vs. ideal acceleration PSD spectra.

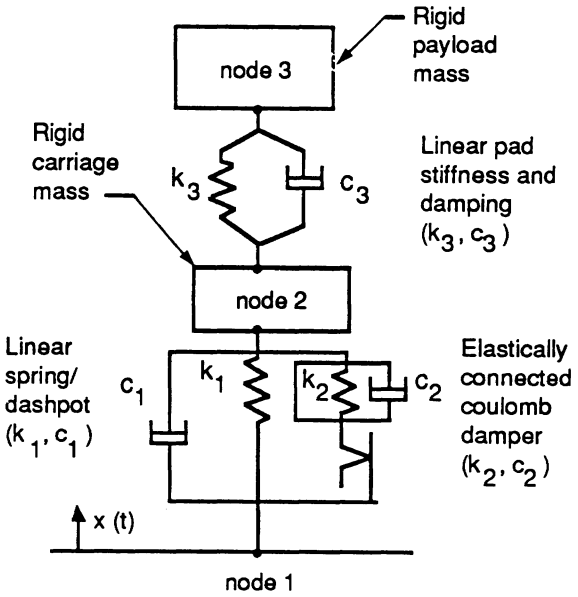

FIGURE 10 Two DOF payload/carriage model.

Description of Model

A two DOF collinear mathematical model representing the nonlinear isolation system connected to the carriage and primary payload masses is shown in Fig. 10. Increasing the DOF for internal payload structural design details does not yield a considerable improvement in the determination of the transmissibility characteristics of the isolator. Therefore, nodes 2 and 3 shown in Fig. 10 represent the rigid carriage and payload masses, respectively, with only vertical motion allowed so that the fundamental vertical resonance mode of the isolator is captured. Carriage/payload interface pad stiffness and damping was assumed linear. The excitation input $x(t)$ is defined at node 1 along the line of action.

Nonlinear Dynamic Response

An excitation time history, $x(t)$ (Fig. 8), was used as input to the two DOF model. As previously discussed, $x(t)$ denotes the calculated time history generated from a prescribed PSD environment (Fig. 7).

The nonlinear time domain model response in the form of transmissibility, that is, (node 2 response)/(node 1 input), was obtained and transformed to the frequency domain. Figure 11 shows the isolator transmissibility for frequencies up to 50 Hz. The numerical values used to calculate the transmissibility via frequency spectra formulation are as follows: $T = 20$, $\Delta t = 0.01$ s, $\Delta f = 0.05$ Hz, for 2000 time samples.

There are two distinct resonant frequencies appearing in the transmissibility plot (Fig. 11). The first peak occurring at 11.2 Hz represents the nonlinear isolator fundamental damped frequency. The second peak occurring at about 25 Hz corresponds to the carriage/payload interface pad damped frequency.

The accuracy of data represented in Fig. 11 is limited to low frequency because of processing time but is adequate to estimate the nonlinear carriage isolation system characteristics. A considerably improved transmissibility function can be obtained by: tapering the time history function, $x(t)$ at both ends to reduce leakage effects; and processing multiple records and applying ensemble of frequency smoothing (Bendat and Piersol, 1986).

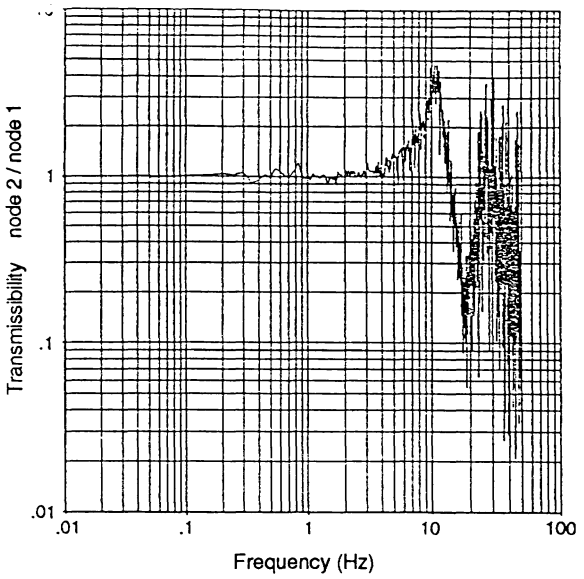

FIGURE 11 Calculated isolator transmissibility function.

Table 1. Equivalent Linear Isolator Definition for T&H Vibration Environments

Vibration Environment	Shock Isolation Frequency (Hz)	Critical Damping (%)
Ground transport		
Primary road at 20 mph	11.9	11.1
Secondary road at 15 mph	11.1	11.1
Air transport		
Runway taxi	11.3	12.5
Runway takeoff and landing	9.5	12.5
Takeoff climb and landing approach	10.9	11.1
Cruise with turbulence	10.9	11.1

DEVELOPMENT OF EQUIVALENT LINEAR ISOLATION SYSTEM

Based on the results of the two DOF nonlinear dynamic analysis, equivalent linear isolator stiffness and damping characteristics (natural frequency, f_n, and percent critical damping ratio, ξ) can be determined corresponding to any given input vibration PSD level. For the case of demonstrated environment $x(t)$, the calculated isolation parameters were $f_n = 11.28$ Hz and $\xi = 0.125$.

Depending on the level of vibration input, different resonant frequency and damping levels would be expected. To illustrate this point, different input T&H environments were applied to the 2 DOF model with the results shown in Table 1. Note that a resonant frequency range of approximately 9.5–11.9 Hz and a damping range of 11.1–12.5% describe the variation in dynamic characteristics for this isolator subjected to the studied environments.

Description of Finite Element Model

The final step in the analysis cycle was to include the equivalent linear isolator characteristics in a much more detailed finite element representation of the carriage/payload and run the frequency response analysis of the prescribed T&H vibration environments. The carriage/payload selected for this study was a complex 3-D NASTRAN model containing approximately 2700 grid points and 4000 structural elements of various types (beams, bars, rods, plates, and

springs). The acceleration PSD response for each environment at the critical payload internal components was compared to the allowables to assess the final random vibration response. This approach avoided a costly and time-consuming nonlinear finite-element analysis.

CONCLUSIONS

A practical approximate approach was developed for the analysis of output PSD of a general nonlinear system. The mathematical models and the PSD conversion methods developed in this study are demonstrated to be successful in the dynamic analysis of a nonlinear shock isolation system. It can be concluded from the study of the numerical results presented here that the two DOF payload/carriage model with the nonlinear isolator element is adequate for a simple but accurate dynamic analysis of an aerospace shock isolation system. The accuracy of the nonlinear isolator element has been demonstrated by comparing predicted responses to test data. The validity of the proposed method for analyzing nonlinear systems can be further supported by performing Monte Carlo simulations. For the highly nonlinear systems where the Gaussian assumption is unjustified, an improved input/output spectral relation is required for predicting the spectral response.

The advantage of first using the simplified models and PSD conversion suggested here prior to the more complex finite-element model approach is that the payload model developed here may include several nonlinear elements that cannot be easily considered in the finite element model. Therefore, following the general technique presented here, the detailed finite-element payload model can be employed with its nonlinear elements replaced by their linear equivalents for the final modal frequency and shock spectrum response analyses.

This work was conducted in support of the U.S. Air Force Ballistic Missile Organization under the Rail Garrison BT&SS Contract No. F04704-87-C-0108. The author wishes to thank the Air Force and The Boeing Company for permission to publish this article. The author also wishes to thank his colleagues Lee J. Favour, Wesley R. Bruner, and Dr. Karlheinz Eisinger for their technical assistance, and Risë A. Windell for preparation of the manuscript.

REFERENCES

Bendat, J. S., and Piersol, A. G., 1986, *Random Data Analysis and Measurement Procedures,* 2nd ed., John Wiley, New York.

Nayfeh, A. H., and Mook, D. T., 1979, *Nonlinear Oscillations,* John Wiley, New York.